Simultaneous Measurements of Actin Filament Turnover, Filament Fraction, and Monomer Diffusion in Endothelial Cells

J. L. McGrath,*† Y. Tardy,§ C. F. Dewey, Jr.,† J. J. Meister,§ and J. H. Hartwig*

*Division of Experimental Medicine, Brigham and Women's Hospital, Boston, Massachusetts 02115 USA; †Fluid Mechanics Laboratory, Department of Mechanical Engineering, Massachusetts Institute of Technology, Cambridge, Massachusetts 02139 USA; and §Biomedical Engineering Laboratory, Swiss Federal Institute of Technology, 1015 Lausanne, Switzerland

ABSTRACT The analogous techniques of photoactivation of fluorescence (PAF) and fluorescence recovery after photobleaching (FRAP) have been applied previously to the study of actin dynamics in living cells. Traditionally, separate experiments estimate the mobility of actin monomer or the lifetime of actin filaments. A mathematical description of the dynamics of the actin cytoskeleton, however, predicts that the evolution of fluorescence in PAF and FRAP experiments depends simultaneously on the diffusion coefficient of actin monomer, D, the fraction of actin in filaments, FF, and the lifetime of actin filaments, τ (Tardy et al., 1995, *Biophys. J.* 69:1674–1682). Here we report the application of this mathematical model to the interpretation of PAF and FRAP experiments in subconfluent bovine aortic endothelial cells (BAECs). The following parameters apply for actin in the bulk cytoskeleton of subconfluent BAECs. PAF: $D = 3.1 \pm 0.4 \times 10^{-8}$ cm^2/s, $FF = 0.36 \pm 0.04$, $\tau = 7.5 \pm 2.0$ min. FRAP: $D = 5.8 \pm 1.2 \times 10^{-8}$ cm^2/s, $FF = 0.5 \pm 0.04$, $\tau = 4.8 \pm 0.97$ min. Differences in the parameters are attributed to differences in the actin derivatives employed in the two studies and not to inherent differences in the PAF and FRAP techniques. Control experiments confirm the modeling assumption that the evolution of fluorescence is dominated by the diffusion of actin monomer, and the cyclic turnover of actin filaments, but not by filament diffusion. The work establishes the dynamic state of actin in subconfluent endothelial cells and provides an improved framework for future applications of PAF and FRAP.

INTRODUCTION

Actin assembly is the basis for shape changes during cell crawling, spreading, and activation. A host of cytoplasmic regulators of actin assembly have been identified. Among these are monomer sequestering proteins (e.g., β4 thymosin, profilin) that prevent assembly at the "pointed" filament end (defined with respect to the stereospecific binding of myosin S1 to actin) and proteins that block monomer access to the fast growing or "barbed" ends of actin filaments (e.g., capZ, gelsolin). The activities of actin-associated proteins and the chemical environment of the cytoplasm results in a steady state in which roughly half of the cellular actin is maintained in an unpolymerized form, with the remainder in a dynamic polymer phase. Cell crawling is achieved by coupling the polymerization of actin filaments in the protruding regions of the cell with filament disassembly in regions of the cell being withdrawn. The lifetime of filaments in cytoplasm is therefore a key determinant of the rate at which cells crawl (Theriot and Mitchison, 1991, 1992).

Estimates of actin filament turnover in living cells (Theriot and Mitchison, 1991, 1992; Wang, 1985; Finkel et al., 1994) are 10–100 times faster than purified actin in vitro (Wegner, 1976). Recently, independent efforts have demonstrated that ADF-cofilin accelerates the depolymerization of actin filaments fivefold in *Xenopus* egg extracts infected with *Lysteria monocytogenes* (Rosenblatt et al., 1997; Carlier et al., 1997) and by an order of magnitude in purified actin filaments (Carlier et al., 1997). Although these in vitro studies have helped resolve a critical disparity between the dynamics of actin in vivo and in vitro, it remains important to improve upon techniques for the assay of actin dynamics in living cells.

The dynamics of actin in living cells has been observed with the techniques of fluorescence recovery after photobleaching (FRAP) and photoactivation of fluorescence (PAF). In these experiments a fluorophore-labeled actin derivative is microinjected into living cells, where it is incorporated into the native cytoskeleton (Amato and Taylor, 1986; Kreis et al., 1979). In FRAP, the fluorescence derived from the injected actin is quenched locally under intense laser excitation. In PAF, a focused band of UV excitation converts a nonfluorescent fluorophore derivative (a "caged" fluorophore) back to its fluorescent parent (Mitchison, 1989). In both techniques the evolution of fluorescence in the illuminated region is monitored to infer information about actin dynamics. While there are theoretical advantages in the signal-to-noise characteristics of PAF compared to FRAP (Krafft et al., 1986), the techniques are otherwise simple inverses of each other.

FRAP experiments on rhodamine and fluorescein-labeled actin have revealed two distinct mobilities of actin. The more mobile phase accounts for 20–80% of the total fluorescence recovery and has been interpreted as the diffusion of actin monomer, monomer/protein complexes, and/or short filaments (Kreis et al., 1982; Luby-Phelps et al., 1985;

Received for publication 15 January 1998 and in final form 2 June 1998.

Address reprint requests to Dr. John H. Hartwig, Experimental Medicine, Brigham and Women's Hospital, 221 Longwood Ave., LMRC Bldg., Boston, MA 02115. Tel.: 617-278-0323; Fax: 617-734-2248; E-mail: hartwig@calvin.bwh.harvard.edu.

0006-3495/98/10/2070/09 $2.00

Wang et al., 1982). The less mobile phase has been attributed to filament remodeling via monomer exchange between filaments and the monomer phase (Wang, 1985). In contrast to FRAP studies, previous PAF experiments exhibit a single decay phase that has been attributed exclusively to filament turnover (Theriot and Mitchison, 1991, 1992). The contrast in the behavior of PAF and FRAP experiments may be due to differences in cell types and the location of photoactivated/photobleached regions within cells; however, differences in the PAF/FRAP techniques or in the application and interpretation of these techniques may also contribute.

Traditionally, FRAP studies on the dynamics of cellular actin have been interpreted using the model of Axelrod et al. (1976). The Axelrod model considers a single diffusive species and an "immobile fraction" and thus is not strictly applicable to experiments on actin, which has two dynamic components. The model of Tardy et al. (1995) describes the spatial and temporal evolution of a PAF experiment in which a diffusive monomer pool exchanges subunits with a nondiffusing polymer (Tardy et al., 1995), providing a more appropriate framework for interpreting PAF and FRAP experiments. The Tardy model produces simultaneous measurements of three important quantities: the diffusion coefficients of actin monomer, D; the fraction of actin in filamentous form, FF; and the turnover time (characteristic lifetime) of actin filaments, τ.

This paper demonstrates application of the Tardy model to PAF and FRAP experiments in the bulk actin cytoskeleton of subconfluent bovine aortic endothelial cells (BAECs). Both PAF and FRAP experiments exhibit biphasic behavior, with an early phase consistent with the diffusion of actin monomer and a second phase consistent with the turnover of actin filaments. Filament diffusion does not appear to contribute significantly to the evolution of fluorescence. Results indicate that actin filament turnover, τ, is rapid (4–8 min) but not diffusion limited in the bulk cytoplasm of endothelial cells. Data are also consistent with previous observations that the mobility, D, of actin monomer differs between cysteine- and lysine-labeled derivatives (Giuliano and Taylor, 1994), and is hindered beyond expectations for a inert tracer of similar hydrodynamic radius (Luby-Phelps et al., 1987).

MATERIALS AND METHODS

Cell culture

Primary cell lines of BAECs were used in both the PAF and FRAP studies. The BAECs employed in Boston for PAF studies were generously supplied by Dr. M. A. Gimbrone (Vascular Research Division, Brigham and Women's Hospital, Boston). BAECs used for FRAP studies in Lausanne were obtained from freshly excised aortas according to the protocol of Booyse et al. (1975). Both lines were grown in Dulbecco's modified Eagle medium (DMEM) with 10% bovine calf serum, 50 units penicillin/streptomycin (1:1), and 1% L-glutamine. BAECs maintain a highly motile phenotype while subconfluent. To ensure the motile phenotype, cells were plated at low density and examined within 2 days of plating. Time-lapse video microscopy of BAECs confirmed that >90% of cells are motile under these conditions, with rms velocities of 0.53 ± 0.094 μm/min (n = 26).

Derivatized actin was microinjected into cells at 5–15% cell volume, and allowed to incorporate for a minimum of 1 h. Cells were maintained at 37°C in observation media (Leibovitz's L-15 with no phenol red, 10% bovine calf serum, 50 units penicillin/streptomycin (1:1), 1% L-glutamine). Exogeneous actin constituted less than 1% of the total actin in injected cells. No differences in the morphology or motile properties were observed in the experimental cells.

Electron microscopy

BAEC monolayers on glass coverslips were permeabilized for 2 min at 37°C by adding a large excess of a solution composed of PHEM buffer 0.06 M PIPES, 0.025 M HEPES, 0.01 M EGTA, 2 mM $MgCl_2$, 0.75% Triton X-100, 1 μM phallacidin, 5.2 nM leupeptin, 1 nM benzamidine, and 12.3 nM aprotinin (Schliwa et al., 1981). The cytoskeletons were fixed for 10 min with PHEM containing 1% glutaraldehyde and 0.1 μM phallacidin. Cytoskeletons were rinsed with PHEM buffer, washed extensively with distilled water, rapidly frozen on a helium-cooled copper block, freeze-dried at −80°C (CFE-50 freeze-fracture apparatus; Cressington, Watford, England) and rotary coated with 1.4 nm of tantalum-tungsten at an application angle of 45°, followed by 5 nm of carbon applied at 90° without rotation. The metal replicas were floated from the coverslips, washed in water, and picked up on carbon-formvar-coated copper grids. Replicas were viewed and photographed in a JEOL 1200-EX electron microscope, using an accelerating voltage of 100 kV.

Actin preparation and injections

Caged-resorufin iodacetamide (CRI) was prepared according to the method of Theriot and Mitchison (1991). Actin was prepared from rabbit skeletal muscle according to the protocol of Spudich and Watt (1971). F-actin was labeled at Cys^{374} with CRI overnight in 10 mM HEPES, 2 mM $MgCl_2$, 100 mM KCl, 0.5 mM ATP (pH 7.8). Caged-resorufin iodacetamide actin (CRIA) was cycled twice between G buffer (2 mM TRIS, 0.2 mM CaCl2, 0.5 mM β-mercaptoethanol, 0.5 mM ATP, pH 7.5) and F buffer (0.1 M KCl, 5 mM $MgCl_2$, 0.1 mM EGTA, 0.5 mM ATP, 10 mM TRIS, 0.5 mM β-mercaptoethanol, pH 7.5) before a final dialysis against G-injection buffer (1 mM HEPES, 0.2 mM $MgCl_2$, 0.2 mM ATP, pH 7.5). The final labeled actin preparation (CRIA) was found to be >95% polymerization competent in vitro with a critical concentration of 0.16 μM. The monomer and polymerized forms of CRIA do not exhibit significant differences in fluorescence at pH 7.5.

For FRAP studies, 5- (and 6) carboxyfluorescein succinimidyl ester-labeled actin (CFSA) was purchased from Cytoskeleton (Denver, CO). CFSA is labeled at lysine and is >90% polymerization competent. From fluorimetery studies, we estimate that CFSA actin is 11% less fluorescent once polymerized at pH 7.5. This was not taken into account in the interpretation of FRAP data because the result could not be verified in cells. If the fluorescence difference does occur in cells, FRAP estimates of FF would be systematically underestimated by 10%, whereas estimates of D and τ would be biased by less than 1%.

PAF experiments

PAF studies were conducted under a modified epifluorescence microscope equipped with two mercury arc lamps. The excitation frequency of resorufin (575 nm) was extracted from one lamp. A second lamp used for uncaging was focused through a rectangular slit and a 390-nm low-pass filter onto the sample plane via a Zeiss 63× plan neofluor objective. The width of the slit in the sample plane varied between 4 μm and 8 μm, and the height of the band spanned a cell in one dimension. Images were acquired in real time with a Hamamatsu CCD coupled to a Video Scope GEN IV intensifier. That the camera/intensifier combination was linear was verified by imaging experimental light levels through a series of

neutral density filters. The lag time of the intensifier/CCD system was studied and found to be negligible in comparison to real-time video integration rates. Both light paths were equipped with electronic shutters. Image acquisition and control of shutters were accomplished with an Apple Macintosh 9500 equipped with a Scion AG-3 framegrabber with digital-to-analog conversion capabilities. The sequence of light exposures and image acquisitions was coordinated with macros developed for the public domain software NIH Image (v 1.61, developed at the U.S. National Institutes of Health and available by anonymous FTP from zippy.nimh.nih.gov). The macros estimate the average fluorescence at the center line of the slit (defined by a region of interest of ~50 pixels (≈19 μm) high × 4 pixels (≈1.5 μm) wide, and sample the background light intensity in a region away from the cell to ensure steady light levels. Uncaging times were adjusted between 250 ms and 1 s as needed for a strong signal. Diffusion coefficients were independent of sampling exposure times in this range, indicating that the longer exposures did not compromise results. The time between the closing of the uncaging shutter and the first sampling point was 67 ms. Cells were exposed to excitation light for 80 ms to acquire a data point.

FRAP experiments

A computer-controlled laser scanning microscope (LSM410; Zeiss, Germany) was programmed to generate a bleaching/imaging sequence. A 15-mW argon laser (488 nm) was passed through a 63× Zeiss plan neofluor objective. The laser was set to 50% maximal power for bleaching and 2% maximal power for imaging. In 300 ms the laser bleached a 3–7-μm rectangular band that spanned one dimension of the cell. The time lag between the bleaching period and the first image was 40 ms. Bleaching and imaging were accomplished by raster scanning the laser across the desired areas. A 10% transmission neutral density filter and a 515-nm high-pass filter were positioned in front of a photomultiplier that recorded the fluorescence as the laser scan was performed. Images were stored and analyzed with the software controlling the microscope. An average fluorescence was computed in the centerline of photobleached bands (~250 pixels high (≈25 μm) × 6 pixels (≈0.5 μm) wide).

Photobleaching controls and corrections

The fluorophore resorufin is highly photolabile under the light levels required to detect it in cells with our intensified CCD. To minimize photobleaching contributions to the fluorescence decay in PAF experiments, the excitation light levels were minimized, the number of data points was limited to 10, and the excitation light was precisely shuttered so that the sample was exposed to light for only 80 ms per data point. To estimate contributions from photobleaching, a control experiment was conducted immediately after a PAF experiment. In the control experiments the entire contents of a cell were uncaged to eliminate the local gradients that generate decay due to diffusion and/or turnover. Images were then acquired with the same exposure times and light intensities as in the experiment. The fluorescence in the region defining the original band centerline was monitored to infer the photobleaching contribution. As shown in Fig. 1 *a*, the photobleaching error accumulated with each exposure and was generally not negligible. When the control experiment is processed through the corrective algorithm given in Appendix A, the effects of bleaching are removed. When the actual experiment is processed through the control, the correction of the data is slight but it is important to a quantitative analysis. The correction is particularly important for estimating the long-term dynamics where the error accumulates. The photobleaching correction assumes that under continuous illumination, photobleaching curves are well approximated by an exponential decay. This behavior is demonstrated for resorufin in Fig. 1 *b*.

At the conclusion of a FRAP experiment, a sequence of images was acquired in which the entire area of the cell was scanned under imaging conditions. The duration of the scan was equivalent to the scanning time used during the actual experiment. The fluorescence in the region of the recovered band was monitored as a photobleaching control. The photobleaching correction algorithm of Appendix A was applied to FRAP data; however, in most cases photobleaching corrections of FRAP data were negligible.

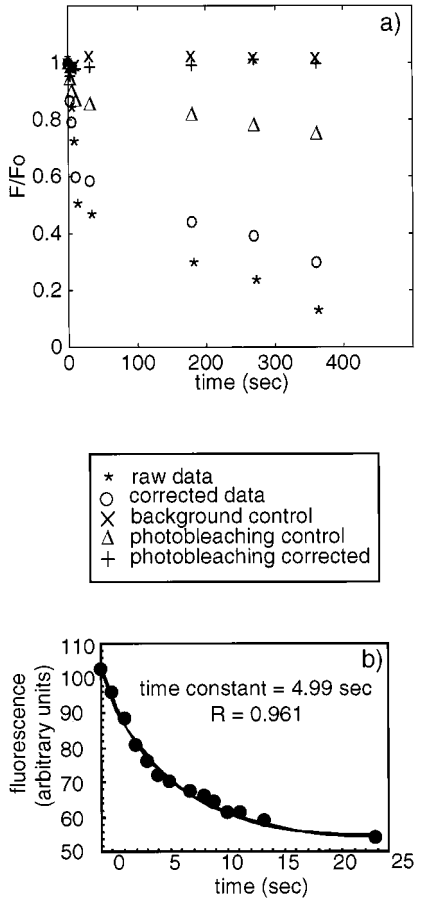

FIGURE 1 Photobleaching and background controls in PAF experiments. After a PAF experiment, microinjected actin throughout the cell is uncaged and a second series of exposures is taken. The decay of fluorescence in the region of the original band is measured as a photobleaching control. (*a*) Raw PAF data (⋆), corrected PAF data (photobleaching control (Δ), corrected control (+), and background control to ensure stable excitation (×). The effects of photobleaching are completely removed from the photobleaching control and the experimental data from the corrective algorithm of Appendix A. The corrective algorithm assumes an exponential photobleaching decay during the 80-ms sampling exposures. (*b*) Demonstration that under continuous illumination, resorufin photobleaching is well approximated by a decaying exponential.

Analysis

The published form of the model of Tardy et al. (1995) is written for a PAF interpretation. Briefly, the fluorescence, F, at time t normalized with respect to the initial fluorescence is given by

$$\frac{F}{F_0} = \frac{1}{1+\gamma}\left(C_m^* + \gamma C_f^*\right) \tag{1}$$

where γ is the local ratio of actin monomer to polymer, C_m^* is the local concentration of fluorescent actin monomer, and C_f^* is the local concentration of fluorescent monomer in filaments. The fluorescent actin concen-

trations are given by the Fourier series expansions

$$C_m^* = \frac{\omega}{L} + \sum_{k=1}^{\infty} \overline{C_m^*} \cos k\pi x^* \quad (2)$$

$$C_f^* = \frac{\omega}{L} + \sum_{k=1}^{\infty} \overline{C_f^*} \cos k\pi x^* \quad (3)$$

where ω is the bandwidth, L is the cell length (see geometry considerations), and x^* is the nondimensional position of the band within the cell. The Fourier coefficients $\overline{C_m^*}$ and $\overline{C_f^*}$ are decaying functions of time. Fluorescence data were fit to this system of equations in a least-squares sense. Summations in Eqs. 2 and 3 were carried out in excess of 500 terms. The nondimensional position, x^*, was fixed at 0.5. The FRAP version of the model is derived from the PAF version above by simply subtracting the right-hand side of Eqs. 2 and 3 from unity.

Geometry considerations

A rectangular photoactivated or photobleached band was employed as in previous PAF studies (Theriot and Mitchison, 1991, 1992; Mitchison, 1989). A 3–8-μm-wide strip illuminates 5–20% of the total cellular area of a typical endothelial cell. This leads to a measurable change in the fluorescence throughout the cell as the photoactivated or photobleached band is homogenized over time. The Tardy model assumes a cell of finite dimension and thus accounts for this rising (PAF) or decaying (FRAP) background.

For convenience the geometry assumed in the Tardy model is that of a rectangular band of fluorescent actin within a bounded rectangular cell. Although to a good approximation both the PAF and FRAP experimental set-ups generate rectangular bands within the cell, the assumption of a rectangular cell is not realized. To use the one-dimensional model to interpret PAF experiments in arbitrarily shaped cells, it is necessary to estimate an equivalent cell length, L_{eq}. Because the ratio ω/L is the normalized fluorescence as $t \to \infty$, we define L_{eq} as

$$L_{eq} = \omega\left(\frac{A_c}{A_s}\right) \quad (4)$$

where ω is the width of the band, A_c is the plan view area of the cell, and, A_s is the plan view area of the uncaged band.

Jasplakinolide and cytochalasin D treatments

To confirm that PAF and FRAP experiments were sensitive to monomer diffusion and the cyclic turnover of filaments, experiments were conducted in the presence of the membrane-permeant polymerizing agent jasplakinolide (Jas) (Molecular Probes, Eugene, OR) (Bubb et al., 1994), and the filament barbed end capping agent cytochalasin D (Cyto D) (Sigma Chemical Co., St. Louis, Mo). PAF experiments were conducted in cells incubated with 1 μM Jas for 20 min. FRAP experiments were conducted in cells incubated with 2 μM Cyto D for 20 min. In both cases changes in cell shape occurred and were taken into account in the analysis. The purpose was to strongly perturb the dynamic state of the actin cytoskeleton. The long-term viability of the cells was not a concern.

RESULTS

Both PAF and FRAP experiments exhibit biphasic decay consistent with the presence of two phases of actin

Subconfluent endothelial cells display a homogeneous actin cytoskeleton in the cell body (Fig. 2). PAF and FRAP experiments were conducted in the cell body using 3–8-μm-wide photoactivated/photobleached bands that spanned one dimension of the cell. Both techniques reveal the presence of two dynamically distinct populations of actin. The initial response occurs on a time scale of 10 s, and the long-term decay occurs on the order of several minutes. Example PAF and FRAP image sequences are shown in Fig. 3. Biphasic behavior is seen in the centerline fluorescence data shown in Fig. 3, *a* (*upper right inset*) and *b* (*upper inset*). The diffusive nature of the early response is best seen in PAF images of Fig. 3 *a*, where the fluorescence spreads rapidly from the band throughout the cell.

Estimates of D, FF, and τ by the Tardy model

The evolution of fluorescence in PAF and FRAP experiments was biphasic, indicating the presence of two dynamically distinct populations of actin. Corrected PAF and FRAP data are shown in Fig. 4, *a* and *b*, respectively. Each corrected experiment was fit to the Tardy model to determine D, FF, and τ. All correlation coefficients exceeded 0.91. The parameters for PAF are: $D = 3.1 \pm 0.4 \times 10^{-8}$ cm^2/s ($n = 20$), FF $= 0.36 \pm 0.04$ ($n = 19$), $\tau = 7.5 \pm 2.0$ min ($n = 17$); those for FRAP are: $D = 5.8 \pm 1.2\ 10^{-8}$ cm^2/s ($n = 25$), FF $= 0.50 \pm 0.04$ ($n = 26$), and $\tau = 4.8 \pm 1.0$ min ($n = 26$). The differences in the PAF and FRAP estimates of D, FF, and τ are statistically significant ($p_D < 0.0005$, $p_{FF} < 0.0005$, $p_\tau < 0.025$) (Table 1). For each study a simulated experiment was generated with the Tardy model and average parameter values. These simulations are plotted along with the data in Fig. 4 to demonstrate the quality of the model fit.

PAF and FRAP experiments are sensitive to Jas and Cyto D

To confirm that PAF and FRAP techniques were detecting the diffusion of sequestered monomer and the cyclic turnover of filaments, studies were conducted in the presence of the polymerizing cytotoxin Jas and the barbed end-capping agent Cyto D. Jas induces actin polymerization with an efficiency and mechanism similar to that of phalloidin (Bubb et al., 1994), but is also cell permeant. After a 20-min incubation in 1 μM Jas, actin in photoactivated bands is immobile on short time scales (compare Fig. 5 *a* and 3 *a*). The images in Fig. 5 *b* are typical of the long-term behavior of cells exposed to 1 μM Jas. Jas stabilizes filaments and induces an apparent contraction in the actin cytoskeleton. The average trend exhibited by seven PAF experiments conducted in cells pretreated with Jas is shown in Fig. 4 *a*. The average decay of fluorescence in the first 30 s is less than 12%. A short time after photoactivation, the fluorescence in the band begins to rise because of the apparent constriction of actin in the photoactivated band. The rising fluorescence precludes an analysis of these experiments with the Tardy model.

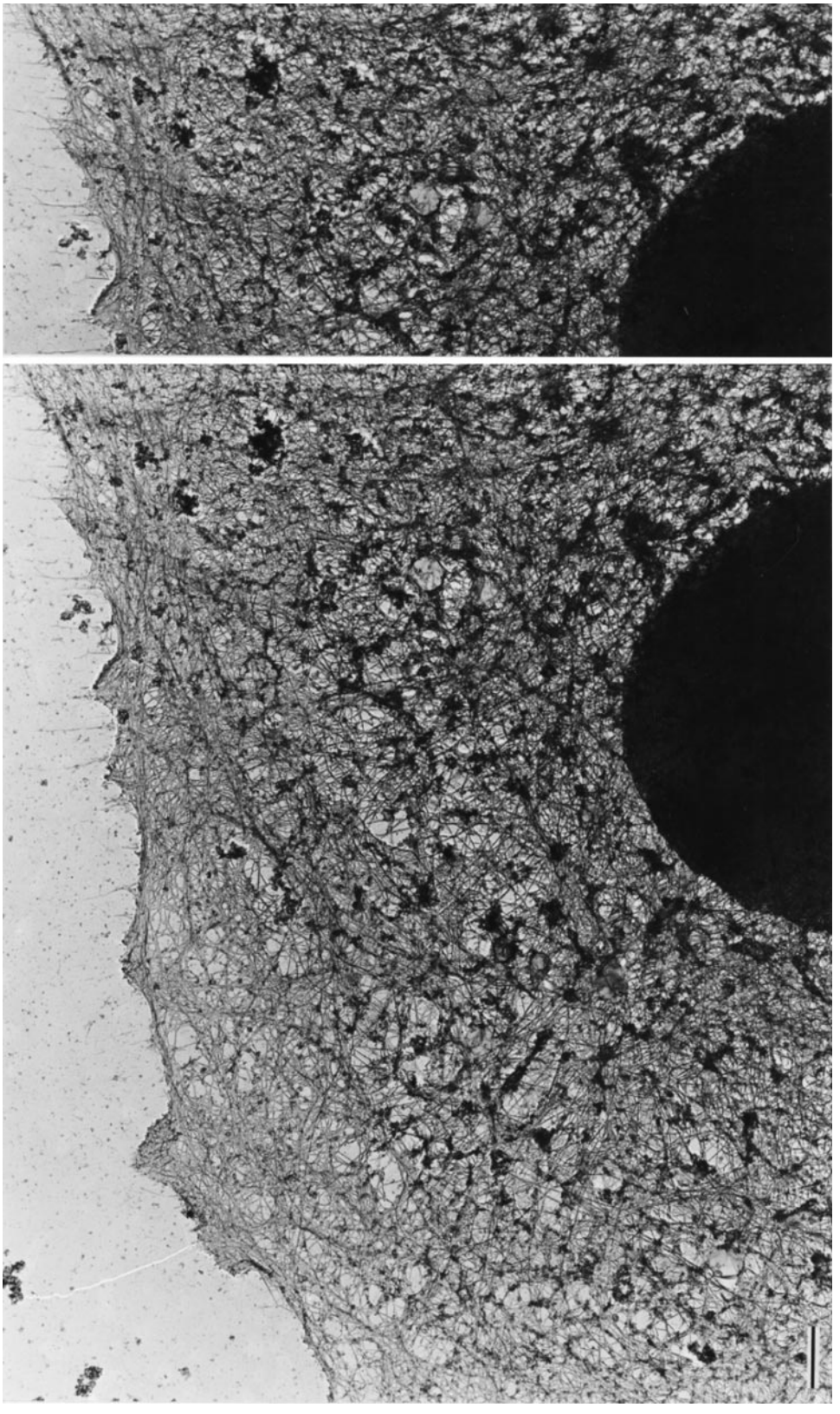

FIGURE 2 Stereo-paired electron micrographs showing uniformity in the actin cytoskeleton. The height of the bottom panel is the nominal width of photoactivated and photobleached regions (7 μm). Photoactivated and photobleached bands traverse the body of the cell, and an average fluorescence is measured along the centerline. Bar = 1 μm.

FRAP experiments were conducted in cells before and after exposure to 2 μM Cyto D for 20 min. Table 2 lists the results of fitting the Tardy model to each of the experiments. The average parameters before and after cytochalasin treatment are (n = 6): $D \pm 3.1 \pm 1.62 \times 10^{-8}$ cm^2/s, FF = 0.42 ± 0.10, $\tau = 4.2 \pm 1.9$ min; and $D = 3.5 \pm 1.7 \times 10^{-8}$ cm^2/s, FF = 0.38 ± 0.09, and $\tau = 20.9 \pm 18.6$ min. A paired t-test indicated that the decrease in FF and the in-

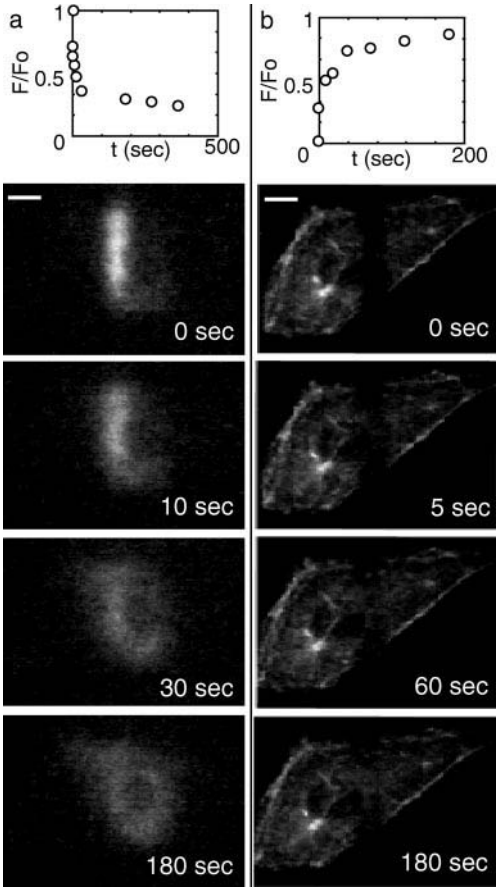

FIGURE 3 PAF and FRAP experiments in BAECs. (*a*) PAF data and associated image sequence. The decay of fluorescence from the photoactivated band is accompanied by a rise in fluorescence elsewhere as monomer diffuses throughout the cell. (*b*) FRAP data and associated image sequence. Both PAF and FRAP data are biphasic, confirming the presence of two dynamic phases. Bars = 10 μm.

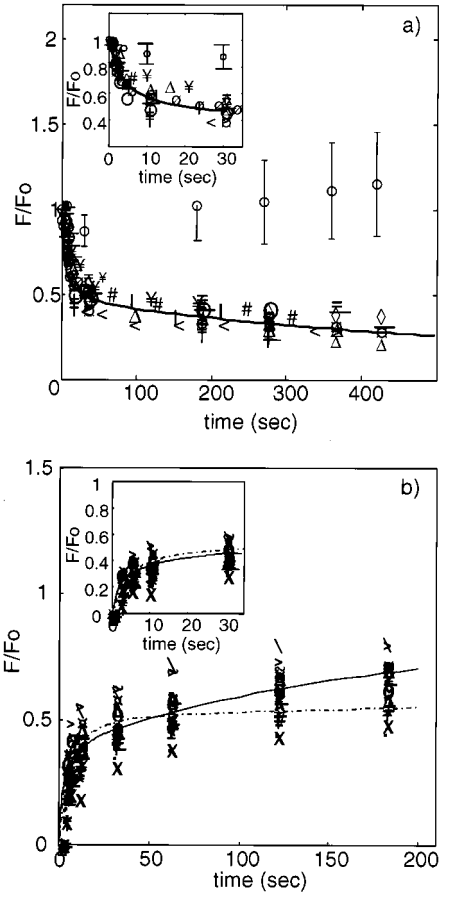

FIGURE 4 PAF and FRAP experiments display biphasic evolution and a sensitivity to actin-targeted drugs. (*a*) Corrected PAF data (20 superimposed experiments) and a curve generated by the average PAF parameter values in Table 1. Also shown is the average evolution of fluorescence in seven cells incubated with Jas for 20 min before photoactivation (○). The error bars indicate mean ± SEM at the respective time points. Jas treatment nearly eliminates the diffusive phase, stabilizes filaments, and results in a rise in fluorescence over time, apparently because of a contraction in the actin cytoskeleton. The inset is a close-up of the short time behavior. (*b*) FRAP data (25 superimposed experiments) and curve produced by the average parameter values in Table 1 (——). Also shown is a curve produced from the average parameter estimates obtained in cells exposed to Cyto D for 20 min (Table 2) before a FRAP experiment (– · –). Cytochalasin decreases the fraction of actin in filaments and slows the turnover of filaments. The inset is a close-up of the short time behavior.

crease in τ are statistically significant ($P_{FF} = 0.059$ and $P_{\tau} = 0.043$), but the slight increase in D is not. A simulated experiment was generated from the mean parameter values after treatment with Cyto D in the Tardy model. This experiment is shown in Fig. 4 *b* for comparison with the data from untreated cells.

DISCUSSION

Cellular actin partitions between a monomer phase, maintained by sequestering proteins such as β4 thymosin and profilin, and a dynamic filamentous phase. The dynamics of an ideal actin tracer should be sensitive to the diffusion of actin monomer, the ratio of monomeric to filamentous actin, the dynamic exchange of monomer between filaments and sequestering proteins, and the diffusion of actin filaments. Because of the high degree of cross-linking exhibited by actin networks in cells (Hartwig and Shevlin, 1986), filament diffusion is predicted to be the smallest contributor to tracer dynamics. With these assumptions, the Tardy model (Tardy et al., 1995) describes the steady-state dynamics of the actin cytoskeleton and predicts the theoretical evolution of fluorescence in a PAF experiment. Here the Tardy model is applied to PAF and FRAP experiments in BAECs to give the first simultaneous measurement of three important parameters in living cells: the diffusion coefficient of actin monomer, D; the fraction of actin in filamentous form, FF: and the lifetime, τ, of actin filaments.

PAF and FRAP experiments in BAECs are biphasic, indicating the presence of two distinct dynamic components. Experiments conducted in the presence of membrane-permeant reagents confirm that these phases are due to monomer diffusion and filament turnover, and not to filament diffusion. First, the high-mobility phase in PAF stud-

TABLE 1 Parameter estimates from PAF and FRAP in BAECs

	$D \times 10^8$ cm^2/s	FF	τ (min)
PAF (CRIA)	3.1 ± 0.4 (n = 20)	0.36 ± 0.04 (n = 17)	7.5 ± 2.0 (n = 17)
FRAP (CFSA)	5.8 ± 1.2 (n = 25)	0.5 ± 0.04 (n = 26)	4.8 ± 0.97 (n = 26)

The uncertainties shown are the standard error of the means. The differences displayed between the two studies are statistically significant, with the following p values obtained from an unpaired t-test. $p_D < 0.0005$, $p_{FF} < 0.0005$, $p_\tau < 0.025$. These differences are attributable to differences in the actin derivative employed with each technique.

ies was nearly eliminated when cells were pretreated for 20 min with 1 μM of the actin-polymerizing reagent Jas, demonstrating that the bulk of this phase is polymerization competent monomer. Second, Cyto D increased the mean estimate of τ by fivefold in FRAP experiments, a result expected for filament turnover but not for filament diffusion. Because cytochalasins block monomer access to the growing (barbed) ends of actin filaments while leaving the depolymerizing (pointed) ends of actin filaments free (Cooper, 1987), depolymerization of filaments proceeds until a new equilibrium is achieved between pointed ends and monomer. Filament turnover via monomer exchange at a single filament end is predicted to be much slower than when both ends are free (Wegner, 1976). Thus the increase in τ with Cyto D is consistent with the assumption that the dynamics of the low-mobility phase are governed by filament turnover. In contrast, filament depolymerization in the presence of cytochalasin should shorten filaments and increase the mobility of the second phase if significant filament diffusion were present.

The following values apply for the bulk actin cytoskeleton in BAECs. PAF: $D = 3.1 \pm 0.4 \times 10^{-8}$ cm^2/s, FF = 0.36 ± 0.04, $\tau = 7.5 \pm 2.0$ min. FRAP: $D = 5.8 \pm 1.2 \times 10^{-8}$ cm^2/s, FF = 0.5 ± 0.04, $\tau = 4.8 \pm 0.97$ min. The differences in the parameters obtained are statistically significant. Cys^{374} labeling of actin (as in CRIA for PAF) results in a derivative with a 10-fold lower affinity for profilin than lysine-labeled derivatives (as in CSFA for FRAP) (Giuliano and Taylor, 1994), and may interfere with the binding of other actin-associated proteins (Kabsch and Vandekerckhove, 1992). Giuliano and Taylor (1994) directly compared the mobility of lysine and Cys^{374}-labeled actin in FRAP experiments in fibroblasts. The estimates of CFSA and CRIA mobility are in good agreement with their values for lysine and Cys^{374}-labeled actin, respectively: $D_{Lys} = 5.6 \pm 1.1 \times 10^{-8}$ cm^2/s (n = 10) and $D_{Cys^{374}} = 3.8 \pm 0.85 \times 10^{-8}$ cm^2/s (n = 10). Furthermore, the filament fractions for CFSA and CRIA agree with the immobile fraction (IF) estimates of Giuliano and Taylor for lysine and Cys^{374}-labeled actin in the peripheral cell body of fibroblasts: $IF_{Lys} = 0.48 \pm 0.04$ (n = 12) and $IF_{Cys^{374}} = 0.34 \pm 0.05$ (n = 13). These agreements suggest that the discrepancies between PAF and FRAP can be largely attributed to differences in the location of fluorophore on actin and not to inherent differences in the techniques. The results indicate that lysine-labeled actin diffuses faster in the cytoplasm, incorporates more readily into the native cytoskeleton, and cycles through filaments faster than Cys^{374}-labeled actin.

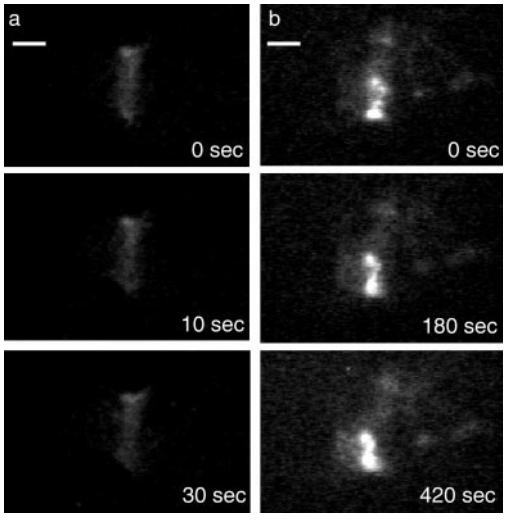

FIGURE 5 PAF sequence after treating cells with 1 μM Jas for 20 min. (*a*) The increased stability of the band at short times demonstrates the conversion of diffusive monomer to filaments. (*b*) PAF sequence in a second cell showing the long-term stability of actin filaments with Jas. Jas stabilizes filaments, but induces an apparent contraction in the cytoskeleton that leads to a rise in the fluorescence in the photoactivated band over time. Bars = 10 μm.

Previously, monomer diffusion coefficients were derived from short-term FRAP data (Kreis et al., 1982; Luby-Phelps et al., 1985; Wang et al., 1982; Taylor and Wang, 1979) by using the protocol of Axelrod et al. (1976). The theory behind the Axelrod protocol considers an inert diffusive phase and a second "immobile" phase and is not strictly applicable to actin, which has two interacting populations. Estimates of D derived from the Axelrod analysis (Luby-Phelps et al., 1985; Giuliano and Taylor, 1994) are at least four times lower than would be expected for an inert particle with the same hydrodynamic radius as monomeric actin (Luby-Phelps et al., 1987). This hinderance is not due to actin binding to known sequestering proteins such as β-4 thymosin and profilin, because these molecules bind actin in 1:1 complexes that have a molecular weight only 10–25% greater than that of actin alone (see Sun et al., 1995, for a review of actin monomer-binding proteins). Because the Axelrod model does not consider filament turnover, an analysis by this model would produce underestimates in D if monomer diffusion were hindered by the cyclic incorporation of monomer into filaments. The Tardy model ac-

TABLE 2 Dynamic parameters in cells before and after treatment with Cyto D

	Baseline			After 20 min in 2 μM Cyto D		
	$D \times 10^8$ cm^2/s	FF	τ (min)	$D \times 10^8$ cm^2/s	FF	τ (min)
Cell 1	3.3	0.38	4.5	2.4	0.30	13.2
Cell 2	3.0	0.32	6.4	6.6	0.38	10.3
Cell 3	2.0	0.38	2.2	3.8	0.36	6.0
Cell 4	6.2	0.40	3.2	3.9	0.28	57
Cell 5	2.1	0.57	2.2	2.1	0.52	26
Cell 6	2.0	0.52	6.4	2.0	0.44	13.6
Mean $\pm$ SEM	3.1 $\pm$ 1.62	0.42 $\pm$ 0.10	4.2 $\pm$ 1.9	3.5 $\pm$ 1.7	0.38 $\pm$ 0.09	21 $\pm$ 9

The differences in FF and τ are statistically significant while the slight increase in D with treatment cytochalasin treatment is not ($p_{FF} = 0.043$ and $p_\tau = 0.059$ determined from a paired t-test).

counts for the influence of filament turnover, yet produces the same estimates for D. This result indicates that filament turnover is too slow to hinder monomer diffusion in the bulk cytoskeleton of BAECs or, equivalently, that filament turnover is not diffusion limited. (For hindrance, the characteristic time of monomer diffusion out of the band must be comparable to or slower than the filament turnover time. This condition holds for $\beta_\omega = \omega^2/\tau D \approx 1$, where ω is the photoactivated bandwidth, D is the diffusion coefficient of actin monomer, and τ is the turnover rate of actin filaments.) Thus although the mobility of actin monomer is restricted in cytoplasm ~15 times from its value in water (Luby-Phelps et al., 1987), monomer diffusion cannot be the limiting factor in determining the time for remodeling of the bulk actin cytoskeleton in BAECs.

Filament turnover times in FRAP or PAF experiments have been estimated from half-lives for the total recovery or decay of fluorescence (Theriot and Mitchison, 1991, 1992; Wang, 1985). Because actin is distributed between monomer and filaments in cells (Bray and Thomas, 1976), the half-life of fluorescence in a PAF or FRAP experiment may not accurately reflect the time scale of either monomer diffusion or filament turnover. For this reason it is not possible to strictly compare the turnover times here to those obtained previously. (Furthermore, our turnover times are not half-lives, but are more accurately thought of as $1/e$ times or the time for the fluorescence due to filaments to decay to 37% of its original value.) Roughly, however, estimates of τ agree with FRAP measurements of filament turnover in the lamellapodia of motile fibroblasts (Wang, 1985), and with recent PAF estimates in the cell body of fibroblasts (Cramer et al., 1997). Our measurements are 1–7 times slower than PAF estimates of τ in the lamellapodia of fibroblasts (Theriot and Mitchison, 1992) and an order of magnitude slower than PAF estimates in the lamellapodia of highly motile keratocytes (Theriot and Mitchison, 1991).

The experiments here establish the general equivalency of the PAF and FRAP techniques when applied to the same cell location and the same cell type. In contrast to FRAP studies in the cell body, however, previous PAF experiments in the lamellapodia of fibroblasts and keratocytes exhibit only a single dynamic component (Theriot and Mitchison, 1991, 1992). A single phase decay in a PAF experiment would indicate that only trace amounts of monomer exist or that the exchange of subunits between monomer and filaments occurs so rapidly that the two phases decay simultaneously. (This is the case of diffusion-limited filament turnover. This condition holds for $\beta_\omega = \omega^2/\tau D \gg 1$.) The ~30-s filament turnover times reported in the lamellapodia of highly motile keratocytes by Theriot and Mitchison (1991) are 2–4 times longer than monomer diffusion times from the 2.5-μm photoactivated band used. Even in this case a biphasic decay of fluorescence would be expected if significant sequestered monomer were present. Thus the disparity between the PAF experiments of Theriot and Mitchison and other studies may indicate a difference in the ratio of sequestered to polymerized actin between the cell body and the lamellapodia.

APPENDIX

The photobleaching process has been successfully modeled as a first-order reaction with a rate constant proportional to the excitation intensity, I (Axelrod et al., 1976):

$$\frac{dF}{dt} = -\eta IF \tag{A1}$$

where F is the fluorescence, and η is a proportionality constant. The final fluorescence of a sample during an exposure to excitation light is given by

$$F_f = (F_i - F_\infty)e^{-\Delta t/\tau} + F_\infty \tag{A2}$$

where Δt is the duration of the exposure, F_i is the sample fluorescence at the beginning of the exposure, and F_f is the sample fluorescence at the end of the exposure. The sample photobleaching time constant τ and the unbleachable background fluorescence F_∞ are estimated from the sample photobleaching decay curve under continuous illumination (see Fig. 1 *b*). The corrected initial fluorescence is given by

$$F_i = \frac{F_f - F_\infty}{e^{-\Delta t/\tau}} + F_\infty \tag{A3}$$

Error due to photobleaching accumulates during an experiment. Defining the drop in fluorescence due to photobleaching during the jth exposure interval as $\Delta F_j = F_{i,j} - F_{f,j}$, the fluorescence at the beginning of the nth ($n \geq j$) exposure interval is corrected for all previous exposures with

$$F_{i,n} = \frac{F_{f,n} - F_\infty}{e^{-\Delta t/\tau}} + F_\infty + \sum_{j=1}^{n} \Delta F_j \tag{A4}$$

Equation A4 is the correction algorithm. If the photobleaching is well characterized by τ and F_∞, substituting measured data (a series of F_f's), in Eq. A4 produces a series of fluorescence values (a series of F_i's) that are void of photobleaching effects.

The authors thank Dr. M. A. Gimbrone for generously providing BAECs and related supplies. Our thanks to M. G. Centeno and Y. Kuang for valuable assistance in cell culture. Thanks to Dr. A. Azim and Mr. C. Hartemink for comments on the manuscript and to Dr. K. Barkalow for discussions and helpful suggestions. Thanks also to Dr. Julie Theriot for the CRIA protocol.

This work was supported by a grant from the CHUV-EPFL-UNIL collaboration program (YT), National Institutes of Health grant HL54145 (JHH and CFD), and by grants from Edwin W. Hiam and the Edwin S. Webster Foundation (JHH). JLM is a Whitaker Foundation Graduate Fellow.

REFERENCES

Amato, P. A., and D. L. Taylor. 1986. Probing the mechanism of incorporation of fluorescently labeled actin into stress fibers. *J. Cell Biol.* 102:1074–1084.

Booyse, F. M., B. J. Sedlak, and M. E. Rafelson, Jr. 1975. Culture of arterial endothelial cells: characterization and growth of bovine aortic cells. *Thromb. Diath. Haemorrh.* 15:825–839.

Bray, D., and C. Thomas. 1976. Unpolymerized actin in fibroblast and brain. *J. Mol. Biol.* 16:1055–1069.

Axelrod, D., D. E. Koppel, J. Schlessinger, E. Elson, and W. W. Webb. 1976. Mobility measurements by analysis of fluorescence photobleaching recovery kinetics. *Biophys. J.* 16:1055–1069.

Bubb, M. R., M. Adrian, J. Senderowiez, E. A. Sausville, L. Kimberly, K. Duncant, and E. D. Korn. 1994. Jasplankinolide, a cytotoxic natural product, induces actin polymerization and competitively inhibits the binding of phalloidin to F-actin. *J. Biol. Chem.* 269:14869–14871.

Carlier, M.-F., V. Laurent, J. Santolini, R. Melki, D. Didry, G.-X. Xia, Y. Hong, N.-H. Chua, and D. Pantaloni. 1997. Actin depolymerizing factor (ADF/cofilin) enhances the rate of filament turnover: implication in actin based motility. *J. Cell Biol.* 136:1307–1322.

Cooper, J. A. 1987. Effects of cytochalasin and phalloidin on actin. *J. Cell Biol.* 105:1473–1478.

Cramer, L. P., M. Siebert, and T. J. Mitchison. 1997. Identification of novel graded polarity actin filament bundles in locomoting heart fibroblasts: implications for the generation of motile force. *J. Cell Biol.* 89: 1287–1305.

Finkel, T., J. A. Theriot, K. D. Dise, G. F. Tomaselli, and P. J. Goldschmidt-Clermont. 1994. Dynamic actin structures stabilized by profilin. *Proc. Natl. Acad. Sci. USA.* 91:1510–1514.

Giuliano, K. A., and D. L. Taylor. 1994. Fluorescent actin analogs with a high affinity for profilin in vitro exhibit an enhanced gradient of assembly in living cell. *J. Cell Biol.* 124:971–983.

Hartwig, J. H., and P. Shevlin. 1986. The architecture of actin filaments and the ultrastructural location of actin-binding protein in the periphery of lung macrophages. *J. Cell Biol.* 103:1007–1020.

Kabsch, W., and J. Vandekerckhove. 1992. Structure and function of actin. *Annu. Rev. Biophys. Biomol. Struct.* 21:49–76.

Krafft, G. A., J. P. Cummings, L. J. Dizig, W. R. Brven, W. R. Sutton, and B. R. Wars. 1986. Fluorescence activation and photodissipation (FDP). *In* Nucleocytoplasmic Transport. Springer-Verlag, New York. 35–52.

Kreis, T. E., B. Geiger, and J. Schlessinger. 1982. Mobility of microinjected rhodamine actin within living chicken gizzard cells determined by fluorescence photobleaching recovery. *Cell* 29:835–845.

Kreis, T. E., K. H. Winterhalter, and W. Birchmeier. 1979. In vivo distribution and turnover of fluorescently labeled actin microinjected into human fibroblasts. *Proc. Natl. Acad. Sci. USA.* 76:3814–3818.

Luby-Phelps, K., P. E. Castle, D. L. Taylor, and F. Lanni. 1987. Hindered diffusion of inert tracer particles in the cytoplasm of mouse 3T3 cells. *Proc. Natl. Acad. Sci. USA.* 84:4910–4913.

Luby-Phelps, K., F. Lanni, and D. L. Taylor. 1985. Behavior of a fluorescent analogue of calmodulin in living 3T3 cells. *J. Cell Biol.* 101: 1245–1256.

Mitchison, T. J. 1989. Polewards microtubule flux in the mitotic spindle: evidence from photoactivation of fluorescence. *J. Cell Biol.* 109: 637–652.

Rosenblatt, J., B. Agnew, H. Abe, J. Bamburg, and T. J. Mitchison. 1997. *Xenopus* actin depolymerizing factor/cofilin (XAC) is responsible for the turnover of actin filaments in *Listeria monocytogenes* tails. *J. Cell Biol.* 136:1323–1332.

Schliwa, M., J. van Blerkom, and K. Porter. 1981. Stabilization of the cytoplasmic ground substance in detergent-opened cells and a structural and biochemical analysis of its composition. *Proc. Natl. Acad. Sci. USA.* 78:4329–4333.

Spudich, J. A., and S. Watt. 1971. The regulation of rabbit skeletal muscle contraction. *J. Biol. Chem.* 246:4866–4871.

Sun, H. Q., K. Kwiatkowska, and H. L. Yin. 1995. Actin monomer binding proteins. *Curr. Opin. Cell Biol.* 7:102–110.

Tardy, Y., J. L. McGrath, J. H. Hartwig, and C. F. Dewey, Jr. 1995. Interpreting photoactivated fluorescence microscopy measurements of steady-state actin dynamics. *Biophys. J.* 69:1674–1682.

Taylor, D. L., and Y. Wang. 1979. Fluorescently labelled molecules as probes of the structure and function of living cells. *Nature.* 284: 405–410.

Theriot, J. A., and T. J. Mitchison. 1991. Actin microfilament dynamics in locomoting cells. *Nature.* 352:126–131.

Theriot, J. A., and T. J. Mitchison. 1992. Comparison of actin and cell surface dynamics in motile fibroblasts. *J. Cell Biol.* 118:367–377.

Wang, Y. 1985. Exchange of actin subunits at the leading edge of living fibroblasts: possible role of treadmilling. *J. Cell Biol.* 101:597–602.

Wang, Y., F. Lanni, P. McNeil, B. Ware, and D. L. Taylor. 1982. Mobility of cytoplasmic and membrane-associated actin in living cells. *Proc. Natl. Acad. Sci. USA.* 79:4660–4664.

Wegner, A. 1976. Head to tail polymerization of actin. *J. Mol. Biol.* 108:139–150.